Migration Letters

Volume: 20, No: S2(2023), pp. 967-978

ISSN: 1741-8984 (Print) ISSN: 1741-8992 (Online)
www.migrationletters.com

Estimation of Deglaciation in the Quillcay River Sub-Basin-Peru, in the Face of Climate Change

Flor Jara[1], Abel Mejía[2], Teófanes Mejía[3], Gerardo Revelo[4]

Abstract

In recent decades, glaciers globally and mainly tropical glaciers have experienced an accelerated retreat of snow cover due to climate change. In the tropical glaciers of Peru, this has generated the development of numerous gaps and an increase in their volume over the years. In the present research, a methodology with new improved indexes is proposed: Normalized Differential Snow Index without water information (NDSInw) and Normalized Differential Water Index without snow information (NDWIns). The changes occurred are identified through a multitemporal analysis of the snow surface in the Quillcay river sub-basin during 1986 to 2021 using satellite images of Landsat 5, 8 and 9 collection 2 of the Google Earth Engine (GEE) data catalog and processing the spatial data using the API (Application Programming Interface) from rgee. The results obtained from the deglaciation of the snow-capped mountains in the 35 years of analysis resulted in a decrease of 27.82% with respect to 1986. The projection of the glacier coverage estimate was made using the linear regression method where the R2 is 0.9614, it was carried out until the year 2056 and the glacier coverage trend is to decrease its volume by 69.5% with respect to the year 1986.

Keywords: *Glacier mass loss, Spectral indices, Remote sensing, Climate change, NDSInw, 1NDWIns.*

1. Introduction

The world of tropical glaciers has retreated during the last century (Rabatel et al., 2013), most of the glacier areas of the world are in constant reduction of their glacier surface. In some there is a partial increase, for example, the Karakoram in the Himalayas where it is manifested by the climatological variations of the place such as the increase of precipitation (Kaltenborn et al., 2010). The main cause of the melting of glacier masses is attributed to the current increase in global temperature due to the consequences of climate change that is affecting different land covers and its progressive change (Mark et al., 2010).

The rapid decline of tropical glaciers has increased awareness of their importance as an important water resource, particularly during the dry season (Bradley et al., 2006; Ebi et al., 2007; Mark et al., 2010). As Andean glaciers retreat, there has been an increase in

[1] Universidad Nacional Santiago Antúnez de Mayolo, Av. Universitaria s/n, Independencia, Huaraz, Ancash, Perú, fjarar@unasam.edu.pe,
Doctorate Program in Water Resources, Universidad Nacional Agraria La Molina (UNALM), Lima, Perú.
[2] Doctorate Program in Water Resources, Universidad Nacional Agraria La Molina (UNALM), Lima, Perú, jabel@lamolina.edu.pe
[3] Universidad Nacional Santiago Antúnez de Mayolo, Av. Universitaria s/n, Independencia, Huaraz, Ancash, Perú, tmejiaa@unasam.edu.pe
[4] Universidad Nacional Santiago Antúnez de Mayolo, Av. Universitaria s/n, Independencia, Huaraz, Ancash, Perú, grevelos@unasam.edu.pe

seasonal discharge and in basins with smaller glacier area and a decrease in total annual discharge (Juen et al., 2007; Mark et al., 2005).

Climate change is altering the entire atmospheric oceanic system globally and mainly in glaciers around the world, being observed with greater susceptibility in the tropical glaciers of the Andes, whose visible result is its deglaciation and accelerated melting in recent decades (Yap Arévalo, 2016). Tropical glaciers are found in greater extension in Peru, hosting about 1200 km2, this makes it have the largest tropical glacier surface at a general level, approximately 71%, of which the Cordillera Blanca comprises 29% representing about 43% with respect to Peru (Rabatel et al., 2013).

Today, access to these tools and to a great diversity of data, such as those obtained by Landsat or Sentinel missions, are indispensable for studies of land cover affected by climate change, such as glaciers. In addition, the use of cloud processing such as that offered by the Google Earth Engine platform makes up for the need to have a large computational platform of its own. Techniques based on remote sensing have proven to be effective tools for detecting changes in land use and changes in the physical environment, quantifying natural ecosystems such as glaciers and cities, providing a comprehensive view of dynamic spaces, utilization models and thus promoting the development of regional development policies (Rogan & Chen, 2004).

2. Method

The development consists mainly in the generation of an algorithm that includes three main steps; 1) Obtaining preprocessed data from satellite images, 2) generation of types of improved terrestrial coverage in spectral indices, 3) extraction of cover class related to glacial lakes and snow cover. After data processing, implementation and analysis of glacier deglaciation was performed.

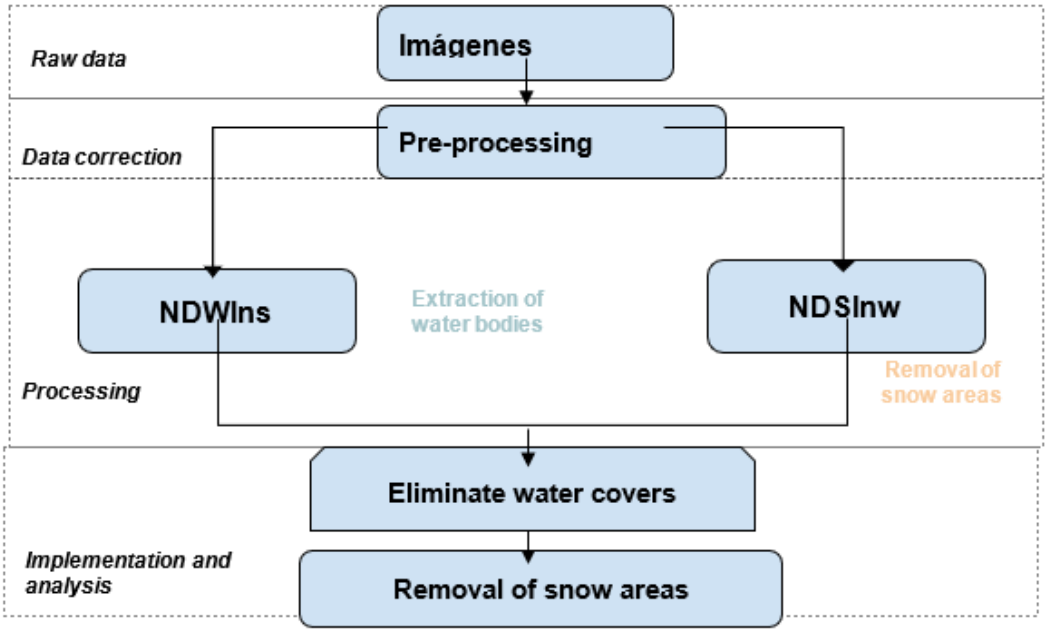

Figure 1: Workflow of the proposed model for snow cover estimation

Source: Authors' elaboration

2.1 Case study and localization

The Cordillera Blanca has the largest glacier area in the tropics (Suárez et al., 2008). The glacier area of the Cordillera Blanca has decreased from 800 - 850 km2 in 1930 to less than 600 km2 at the end of the 20th century (Georges, 2004). Subsequently, glaciers

continued to shrink to reach an area of 482km2 in 2010 (Burns and Nolin, 2014). The region is characterized by heavy seasonal precipitation, which is typical of the outer tropical zone; over 80% of precipitation falls between the months of October and April, with little or no precipitation during the austral winter months of June to August. In the upper Santa River basin, glacial melt (ice and snow melt from glaciers) provides 10 - 20% of the total annual discharge of the river and in the dry season, can exceed 40% (Mark et al., 2005).

The White Cordillera contains about 70% of the world's tropical glaciers. Glacier melt provides 10 to 20% of the total annual discharge of the Santa River, with 40% occurring in the dry season(J.A. Grande et al., 2019). This makes the basin vulnerable to droughts, especially due to an accelerated process of glacial retreat (Mark et al., 2005; Baraer et al., 2009).

The Quillcay river sub-basin is located in the Santa river basin, which is on the Pacific slope. Geopolitically, it is located in the province of Huaraz, district of Huaraz and Independencia. It has an area of 247.38 km2 and a perimeter of 83.03 km. The waters drain along the right bank of the Santa River basin, originating from the Cojup River and forming the Paria River, which joins downstream with the Auqui River and is called Quillcay. The river flows through the main city of Huaraz and empties into the Santa River (Meza et al., 2016).

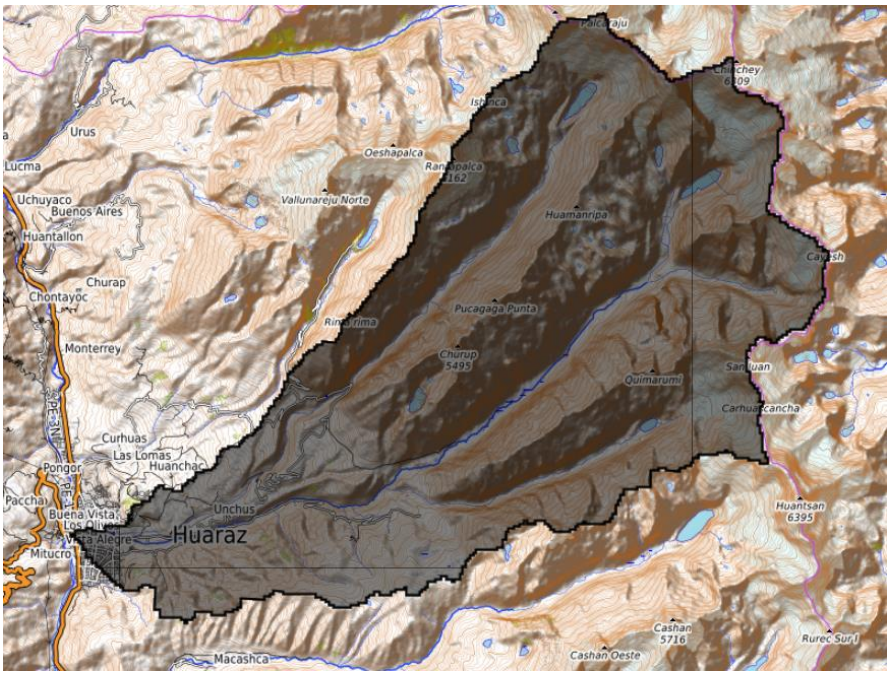

Figure 2. Study area, the Quillcay river sub-basin

Source: Authors' elaboration

2.2 Source of data

The Landsat surface reflectance (SR) corrected time series images are provided by the United States Geological Survey (USGS) and are fully available and ready to use in Google Earth Engine (GEE) for Landsat 4-9, collection 2 which has improved data, processing and algorithm development.

Table 1. Landsat 5, 8 and 9 Collection 2 features

Satellite	Landsat-5	Landsat-8	Landsat-9
Bands of sensors	Band 1 (blue)	Band 1 (coastal aerosol)	Band 1 (ultra blue, coastal aerosol)
		Band 2 (blue)	Band 2 (blue)
	Band 3 (red)	Band 3 (green)	Band 3 (green)
	Band 4 (near infrared)	Band 4 (red)	Band 4 (red)
	Band 5 (shortwave infrared 1)	Band 5 (near infrared)	Band 5 (near infrared)
	Band 6 (Thermal Infrared 1)	Band 6 (shortwave infrared 1)	Band 6 (shortwave infrared 1)
	Band 7 (shortwave infrared 2)	Band 7 (shortwave infrared 2)	Band 7 (shortwave infrared 2)
		Band 8 (Panchromatic)	Band 8 (Panchromatic)
		Band 9 (Cirrus)	Band 9 (Cirrus)
		Band 10 (Thermal infrared 1)	Band 10 (Thermal infrared 1)
		Band 11 (Thermal infrared 2)	Band 11 (Thermal infrared 2)
Spatial resolution	30m	30m	30m
Sensor	TM	OLI-/TIRS	OLI-/TIRS-2
Type of application correction	Surface Reflectance (SR)	Surface Reflectance (SR)	Surface Reflectance (SR)

Source: Authors' elaboration

Landsat imagery provided by GEE contains Multispectral Scanner (MSS) sensors from Landsat 1-5 from 1972 to 1999; Thematic Mapper (TM) from Landsat 4 and 5 from 1982 to 1993; Enhanced Thematic Mapper Plus (ETM+) from Landsat 7 from 1999 to 2021; Operational Land Imager (OLI) and Thermal Infrared Sensor (TIRS) from Landsat 8 from the year 2013 to the present; and recently launched Operational Land Imager 2 (OLI-2) and Thermal Infrared Sensor 2 (TIRS-2) from Landsat 9 from the year 2021 to the present. The Landsat image bands, for the most part, have a spatial resolution of 30m and temporal resolution for the sensors of 16 days.

Table 2: Information and source of images

Quillcay River Sub-basin			
Image	Collection	Cloudiness (%)	Source
Median 1986	LANDSAT/LT05/C02/T1_L2	15	Dataset Earth Engine
Median 1994	LANDSAT/LT05/C02/T1_L2	15	Dataset Earth Engine
Median 1999	LANDSAT/LT05/C02/T1_L2	15	Dataset Earth Engine
Median 2007	LANDSAT/LT05/C02/T1_L2	15	Dataset Earth Engine

Median 2014	LANDSAT/LC08/C02/T1_L2	15	Dataset Earth Engine
Median 2021	LANDSAT/LC08/C02/T1_L2	15	Dataset Earth Engine

Source: Authors' elaboration

2.3. Procedure and application of the methodology

Initially, Landsat 5, 8 and 9 satellite images of the collection 2 of 30 m resolution provided by the Google Earth Engine (GEE) data catalog, the images are corrected at the surface level. The images are surface level corrected. Landsat 5 TM sensor images from 1986, 1994, 1999, 2007, Landsat 8 OLI and TIRS sensors from 2014 and Landsat 9 OLI-2 and TIRS-2 sensors from 2021 were selected. The selected series of images are obtained in the dry season (dry season) from May 1st to September 1st of each year.

A scale factor was applied for the selected images, the factors are different for both Landsat Collection 1 and Landsat Collection 2 Level-2 surface reflectance and surface temperature products. Landsat Collection 2 surface reflectance has a scale factor of 0.0000275 and an additional offset of -0.2 per pixel. For example, a pixel value of 18 639 is multiplied by 0.0000275 for the scale factor and then -0.2 is added for the additional offset to get a reflectance value of 0.313 after applying the scale factor (USGS Landsat 8 Level 2, Collection 2, Tier 1 | Earth Engine Data Catalog | Google Developers, s. f.). The rgee API that integrates Google Earth Engine with R was used and through a script the scale factor for the series of images was applied by creating a calculation function.

Landsat image processing was performed in the cloud using the Google Earth Engine (GEE) platform using a portion of Google's supercomputer.

The images are filtered by date of acquisition for the established years; filtered by study area of the Quillcay river sub-basin, filtering by metadata is established using a cloud cover of less than 15% that allows obtaining clean images without cloud alterations, the scale factor for Landsat 5 and Landsat 8 and 9 together is applied since they have similar scaling for the bands; a median was applied for all the images for each year reducing it to one image, and finally the cut-off for the study area was established.

Landsat 5 (1986)	**Landsat 5 (1994)**
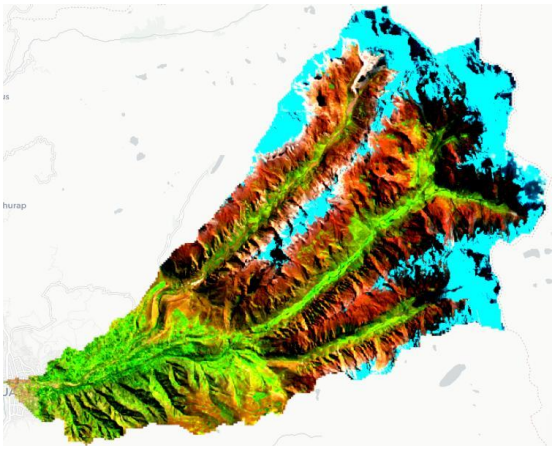	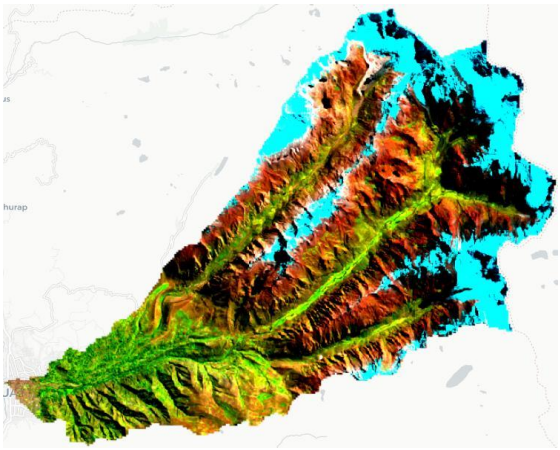
Combination SR_B5, SR_B4 and 'SR_B3'	**Combination SR_B5, SR_B4 and 'SR_B3'**
Landsat 5 (1999)	**Landsat 5 (2007)**

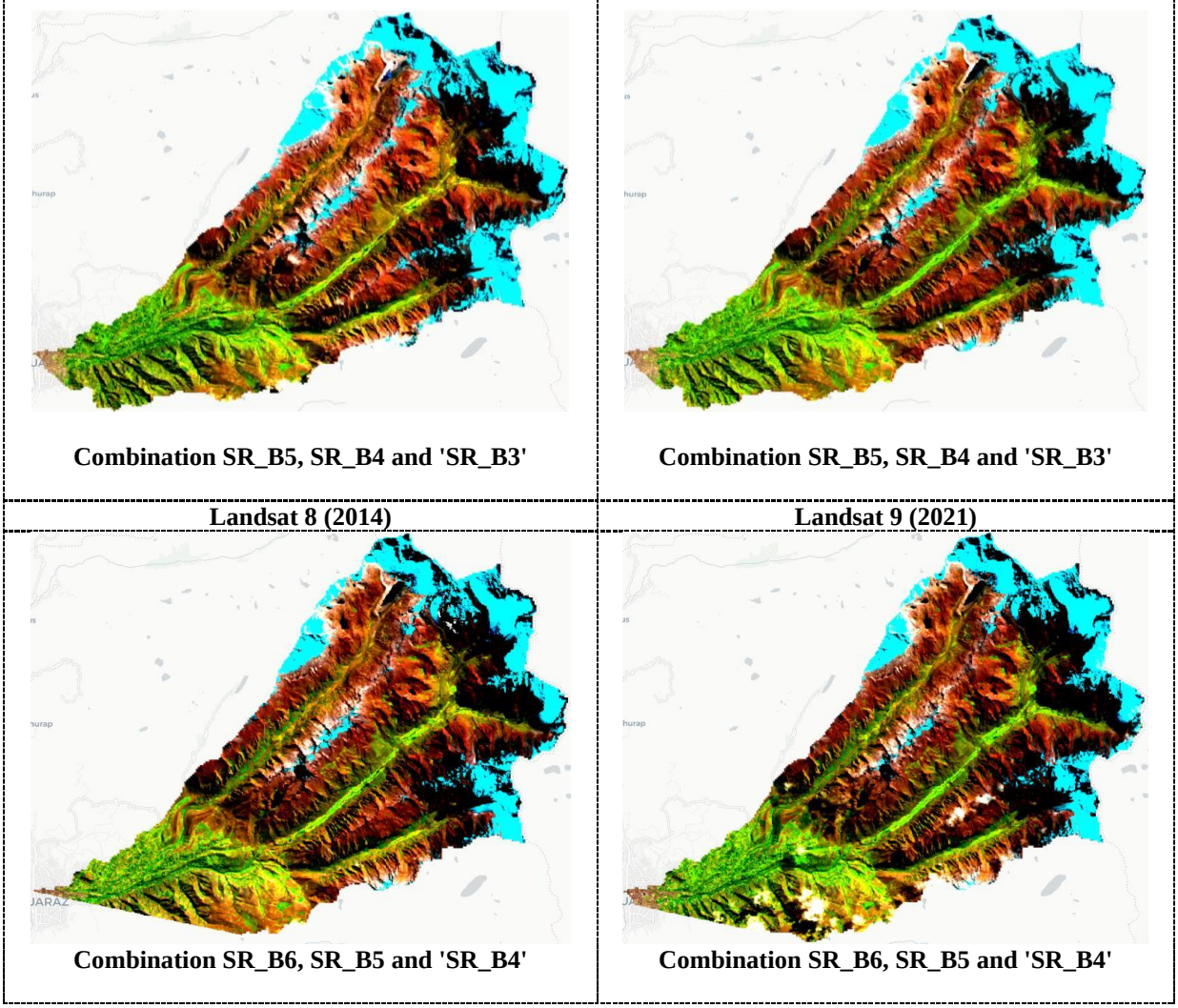

Figure 3. Landsat Collection 2 Surface Reflectance Shortwave Infrared 1, Near Infrared and Red Band Combinations

Source: Own elaboration

The normalized differential equation without water information (NDSInw) was used. The equation uses the near infrared (NIR) band and the short wavelength band 1 (SWIR1). Normalizing the difference between the NIR band and the SWIR1 band keeps the index value high in the snow cover areas and low in the lake water areas.

To further reduce the lake water information, a positive value (0.05) is subtracted from the value of the difference between the NIR band and SWIR1 band. Therefore, NDSInw is proposed to extract snow areas and suppress the noise of lake water bodies to a less relevant level (Yan et al., 2020).

$$NDSInw = (p_{nir} - p_{swir1} - b)/(p_{nir} + p_{swir1})$$

After performing the proposed index, the threshold that obtains the difference between snow and non-snow is 0.4. This threshold typically changes seasonally (Salcedo, 2011).

We propose the normalized differential water index without snow cover (NDWIns). The equation uses the green band and the NIR band remains at a high level in lake water areas, but at a low level in SCG areas. In addition, the contrast values between the lake water and snow bodies are excellent by normalizing the difference between the green band and the NIR band. This index is excellent for eliminating noise generated from

water coverage with the NDSInw index. The empirical parameter that is multiplied to the NIR band, the value of 2 (Yan et al., 2020).

$$NDWIns = (p_{green} - a * p_{nir})/(p_{green+p_{nir}})$$

In the calculation of the different indexes the values obtained are between -1 and 1 and the values that are above 0 means the presence of similar characteristics observed and below the value means the absence or lack of analyzed characteristic. In other words, all positive values from 0 to 1 are considered to represent surfaces with the target features and all negative values from -1 to 0 are considered to be with land of different type of feature (Dolean et al., 2020).

The procedural script of the proposed research methodology can be found here:

https://drive.google.com/file/d/1JOBFcn3_jKudvG05HHQdcEg-lPTj4a4G/view?usp=sharing

Once the area of the glacier surface was obtained for the processing method with Google Earth Engine in Rstudio, the average volume of the glaciers in the sub-basin was estimated with the following formula (Klein & Isacks, 1998):

$$V = C * A^b$$

Where V is glacier volume in km3, A is the area of the glacier surface in km2, the value of C and b as empirical, C= 0,048 and b = 1,36.

3. Results and discussion

Glacier area estimation

The visual representation of glacier deglaciation dynamics in the face of climate change is possible by means of a multitemporal snow cover analysis. The results obtained show the decrease of snow cover in its spatial analysis during 35 years. Applying the methodology proposed for this research, the results of snow cover areas were obtained for 1986, 1994, 1999, 2007, 2014 and 2021 in the Quillcay river sub-basin; the areas of snow cover for the years 1986, 1994, 1999, 2007, 2014 and 2021 in the Quillcay river sub-basin were obtained 41.47 km2, 38.55 km2, 35.16 km2, 32.89 km2, 31.39 km2 y 29.93 km2, respectively, as shown in Figure 4.

Landsat 5 (1986)	**Landsat 5 (1994)**
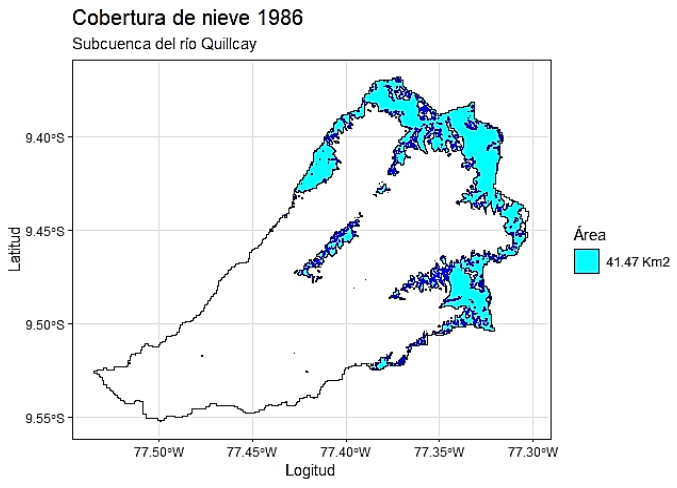	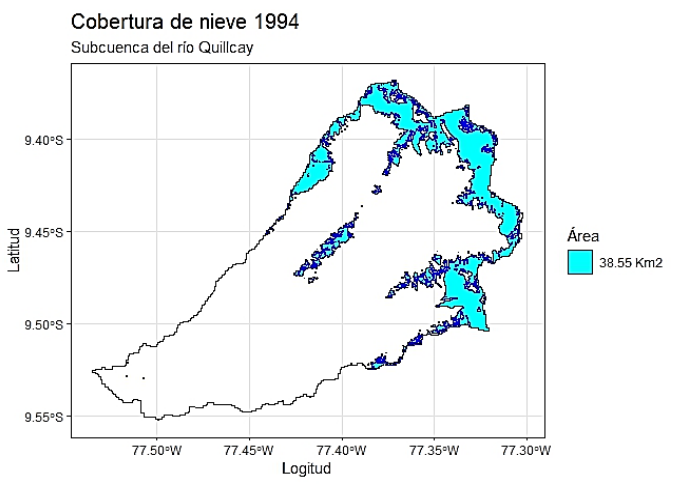
Área: 41.47 km2	**Área: 38.55 km2**

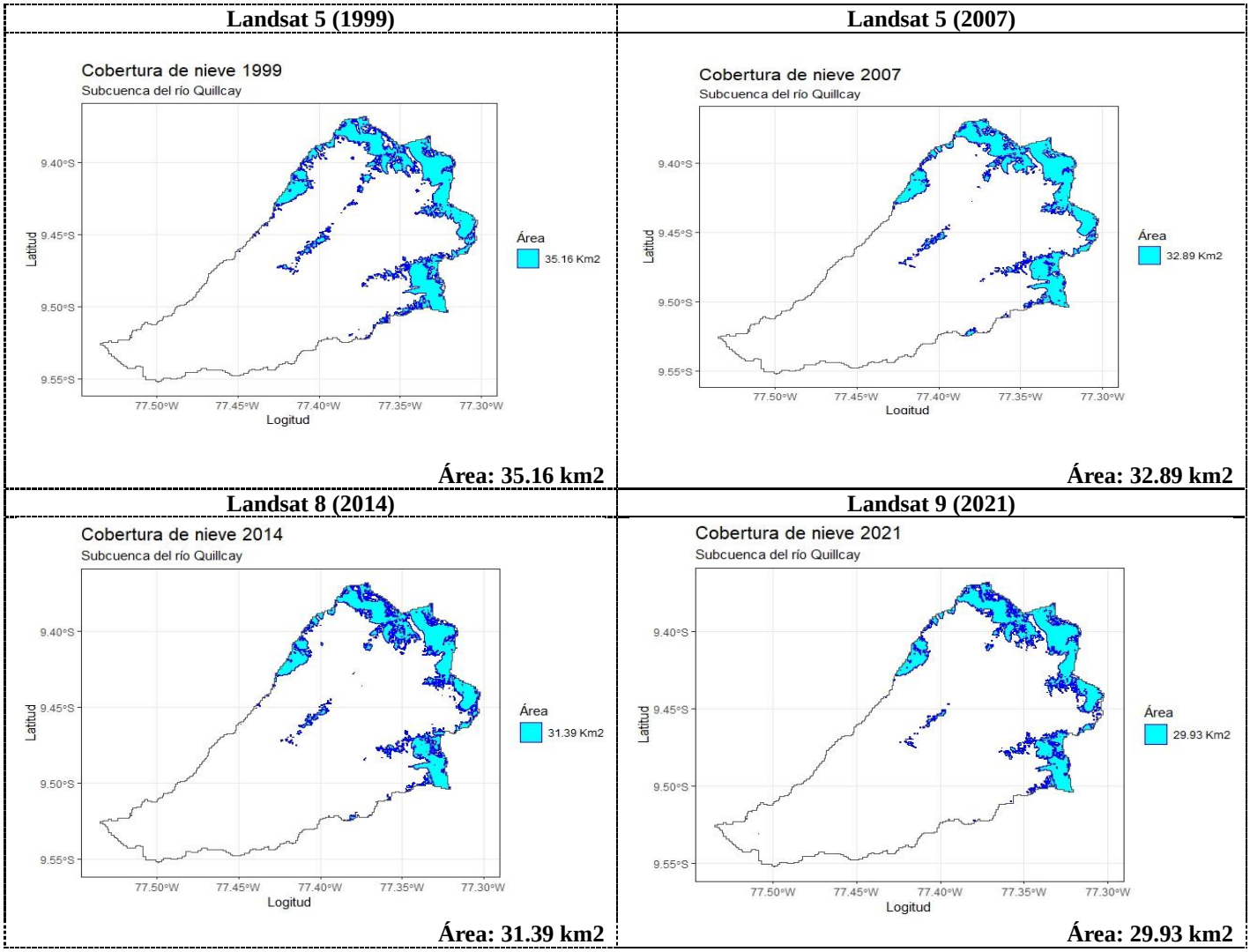

Figure 4. Results of the snow cover analysis from 1986 to 2021

Source: Authors' elaboration

The result of snow cover deglaciation in the 35 years of analysis was a decrease of 27.82% with respect to 1986.

In all the peaks that cover the Quillcay River sub-basin there is a partial decrease in coverage, the drastic decrease in snow cover due to climate change is evident in the coverage of the Huamanripa ravine of 5258 m.a.s.l. and a considerable decrease in the peaks Pucagaga Punta 5461 m.a.s.l., Churup 5495 m.a.s.l. and Cerro Cachijirca, as shown in Figure 5. Churup 5495 m.a.s.l. and Cerro Cachijirca, as can be seen in Figure 5.

To improve the estimation of snow cover for the sub-basin, it is necessary to make a comparison with traditional snow and water calculation indices, such as the Normalized Differential Snow Index (NDSI) and the Normalized Differential Water Index (NDWI) (NDWI).

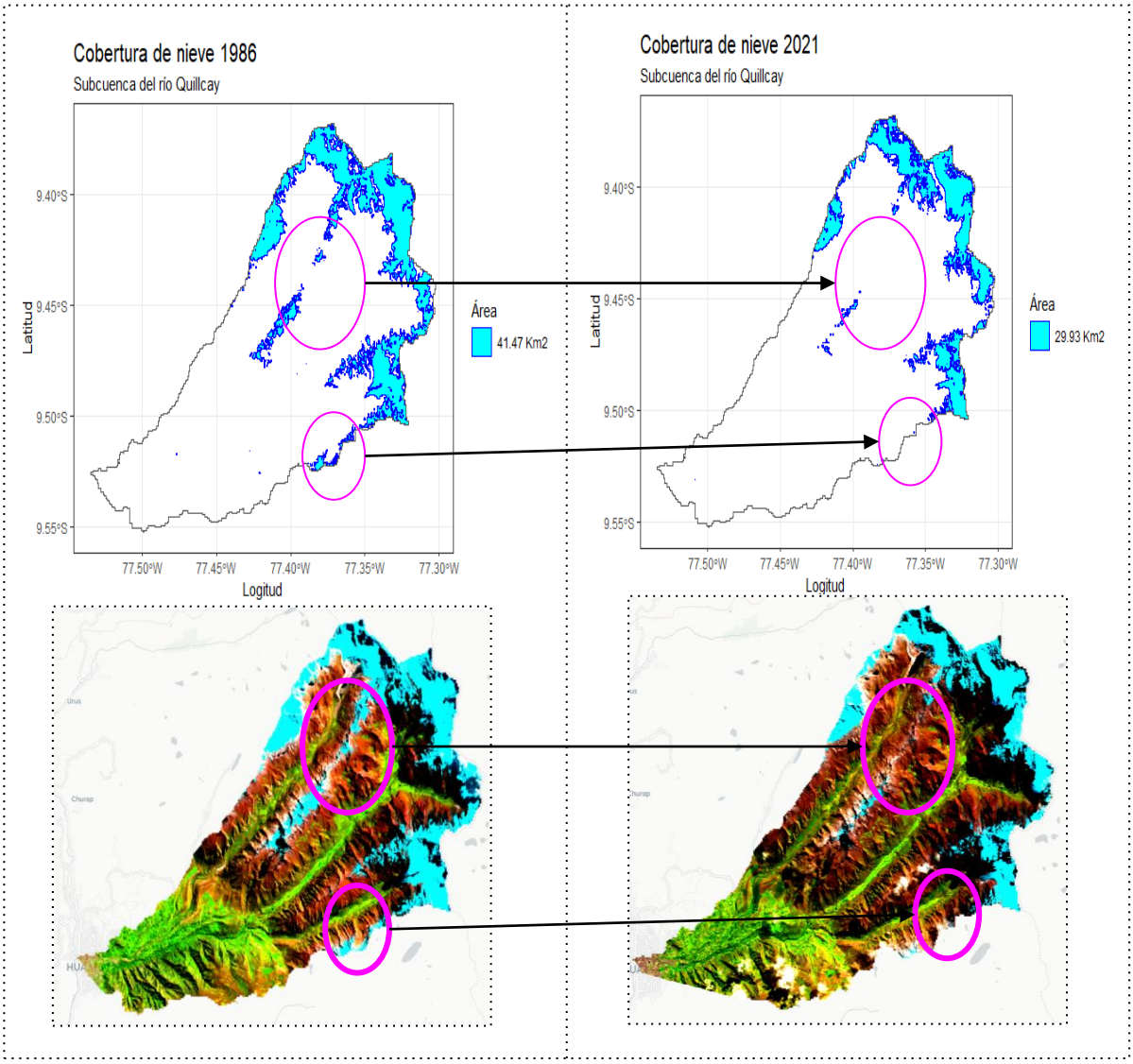

Figure 5. Comparison of snow cover in 1986 and 2021

Source: Authors' elaboration

In addition, other indices such as Normalized Differential Snow and Ice Index (NDSII), Normalized Differential Glacier Index (NDGI) and Normalized Differential Snow and Ice Index (NDSII 2) can be implemented to map ice and snow covers in different classes (Monterroso-Tobar et al., 2018). For more accurate mapping, Machine Learning algorithms such as unsupervised and supervised classifications are implemented, in addition using Convolutional Neural Networks (CNN) as the U-Net model in glacier area estimation (Caillahua & Elbis, 2020).

Quantification of glacier volume

The volume of glaciers in the sub-basin has been decreasing, as shown in Table 2. This quantification of glacier volume shows that the tropical glaciers in the sub-basin lost 2.73 of volume, which represents an average of 36% of glacier melt in the last 35 years of analysis, as can be seen in Table 2 below.

Table 3. Variation of glacier volume in the Quillcay river sub-basin

Quillcay River Sub-basin			
Years	**Area (km^2)**	**Volume (km^3)**	**Percentage (%)**
1986	41.47	7.61	100
1994	38.55	6.89	90
1999	35.16	6.08	80
2007	32.89	5.55	73
2014	31.39	5.21	68
2021	29.93	4.88	64

Source: Authors' elaboration

Table 4. Regression statistics

Regression statistics	
Multiple correlation coefficient	0.9805
Coefficient of determination R^2	0.9614
R^2 adjusted	0.9517
Standard error	0.9709
Observations	6

Source: Authors' elaboration

Projected glacier coverage

For the projection of the glacier coverage estimate, the linear regression method was used, where the R2 is 0.9614. The projection was made until the year 2056 and the trend of glacier coverage is to decrease its volume by 69.5% with respect to 1986 due to the constant deglaciation of glaciers due to climate change.

Table 5. Variation of glacier volume in the Quillcay river sub-basin

Quillcay River Sub-basin			
Years	Area (km2)	Volume (km3)	Percentage (%)
1986	41.47	7.61	100
1994	38.55	6.89	90.55
1999	35.16	6.08	79.89
2007	32.89	5.55	72.96
2014	31.39	5.21	68.47
2021	29.93	4.88	64.18
2028	26.65	4.17	54.81
2035	24.32	3.68	48.39
2042	21.99	3.21	42.19
2049	19.65	2.76	36.22
2056	17.32	2.32	30.5

Source: Own elaboration

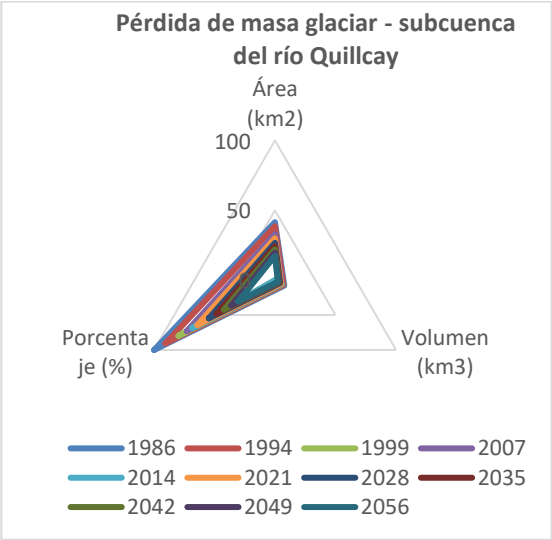

Figure 6. Glacier mass loss

Source: Authors' elaboration

4. Conclusion

There is a trend in the melting of the glaciers in the Quillcay River sub-basin, which is causing an increase in the volume of glacial lakes, mainly due to climate change that has been evident in recent decades.

According to what was proposed in the research, it is considered that it was accomplished, developing an adequate methodology for the analysis of the snow surface for the analysis of deglaciation in the tropical glaciers in the sub-basin of the Quillcay River in the city of Huaraz. In the 35 years of multitemporal analysis with Landsat satellite images from 1986 to 2021, the snow cover surface decreased by 11.54%, which may be related to climate change.

In terms of volume, a total of 2.73 km3 was lost, representing 35.82% of deglaciation in the 35 years of analysis, which may be related to climate change. A projection of the estimated glacier coverage was made using the linear regression method where the R2 is 0.9614, it was carried out until 2056 and the trend of glacier coverage is to decrease its volume by 69.5% with respect to 1986.

The methodology developed can be applied to other high Andean zones of tropical glaciers or polar zones where the territory has glacier coverage related to the cryosphere.

References

Baraer, M.,McKenzie, J.M.,Mark, B.G., Bury, J., Knox, S., 2009. Characterizing contributions of glacier melt and groundwater during the dry season in a poorly gauged catchment of the Cordillera Blanca (Peru). ADGEO 22, 41–49.

Bradley, R.S., Vuille, M., Diaz, H.F., Vergara, W., 2006. Threats to water supplies in the tropical Andes. Science 312, 1755–1756.

Burns P, Nolin A. 2014. Using atmospherically-corrected Landsat imagery to measure glacier area change in the Cordillera Blanca, Peru from 1987 to 2010. Remote Sensing of Environment 140: 165–178.

Caillahua, C., & Elbis, P. (2020). Estimación de área glaciar utilizando Redes Neuronales convolucionales U-Net en imágenes multiespectrales sentinel 2 en el glaciar ausangate, 2019.

Universidad Nacional del Altiplano. http://repositorioslatinoamericanos.uchile.cl/handle/2250/3279796

Dolean, B.-E., Bilașco, Ștefan, Petrea, D., Moldovan, C., Vescan, I., Roșca, S., & Fodorean, I. (2020). Evaluation of the Built-Up Area Dynamics in the First Ring of Cluj-Napoca Metropolitan Area, Romania by Semi-Automatic GIS Analysis of Landsat Satellite Images. Applied Sciences, 10(21), 7722. https://doi.org/10.3390/app10217722

Ebi, K.L., Woodruff, R., von Hildebrand, A., Corvalan, C., 2007. Climate changerelated health impacts in the Hindu Kush–Himalayas. Ecohealth 4, 264–270.

Georges C. 2004. 20th-century glacier fluctuations in the tropical Cordillera Blanca, Peru. Arctic, Antarctic, and Alpine Research 36: 100–107.

Grande J.A, 2019. "The Negro River (Ancash-Peru): A unique case of water pollution, three environmental scenarios and an unresolved issue"

Juen, I., Kaser, G., Georges, C., 2007. Modeling observed and future runoff from a glacierized tropical catchment (Cordillera Blanca, Peru). Global Planet. Change 59, 37–48.

Kaltenborn, B. P., Nellemann, C., & Vistnes, I. I. (2010). High mountain glaciers and climate change: Challenges to human livelihoods and adaptation. GRID-Arendal : UNEP.

Klein A. & Isacks B. 1998. Alpine glacial geomorphological studies in the central Andes using Landsat thematic mapper images. Glacial Geology and Geomorphology; rp01/1998.

Mark, B.G., McKenzie, J.M., Gomez, J., 2005. Hydrochemical evaluation of changing glacier meltwater contribution to stream discharge: Callejon de Huaylas, Peru. Hydrol. Sci. J. 50, 975–987.

Mark, B. G., Bury, J., McKenzie, J. M., French, A., & Baraer, M. (2010). Climate Change and Tropical Andean Glacier Recession: Evaluating Hydrologic Changes and Livelihood Vulnerability in the Cordillera Blanca, Peru. Annals of the Association of American Geographers, 100(4), 794-805. https://doi.org/10.1080/00045608.2010.497369

Meza, H. M., Balabarca, H. V., Pereda, J. R., Rosario, A. M., & Vidal, D. O. (2016). INFORMACION DE CARACTERIZACIÓN DE LA SUBCUENCA DEL RIO QUILLCAY. 14.

Monterroso-Tobar, M. F., Londoño-Bonilla, J. M., & Samsonov, S. (2018). Estimación del retroceso glaciar en los volcanes Nevado del Ruiz, Tolima y Santa Isabel, Colombia a través de imágenes ópticas y Din-SAR. DYNA, 85(206), 329-337.

Rabatel, A., Francou, B., Soruco, A., Gomez, J., Cáceres, B., Ceballos, J. L., Basantes, R., Vuille, M., Sicart, J.-E., Huggel, C., Scheel, M., Lejeune, Y., Arnaud, Y., Collet, M., Condom, T., Consoli, G., Favier, V., Jomelli, V., Galarraga, R., … Wagnon, P. (2013). Current state of glaciers in the tropical Andes: A multi-century perspective on glacier evolution and climate change. The Cryosphere, 7(1), 81-102. https://doi.org/10.5194/tc-7-81-2013

Rogan, J., & Chen, D. (2004). Remote sensing technology for mapping and monitoring land-cover and land-use change. Progress in Planning,61(4),301-325. https://doi.org/10.1016/S0305-9006(03)00066-7

Salcedo, A. P. (2011). Estimación de área cubierta de nieve en cuencas con elevado aporte de fusión utilizando datos ERS-2. https://rdu.unc.edu.ar/handle/11086/6925

Suarez W, Chevallier P, Pouyaud B, Lopez P. 2008. Modelling the water balance in the glacierized Paron Lake basin (White Cordillera, Peru). Hydrological Sciences Journal 53: 266–277.

USGS Landsat 8 Level 2, Collection 2, Tier 1 | Earth Engine Data Catalog | Google Developers

Yan, D., Huang, C., Ma, N., & Zhang, Y. (2020). Improved Landsat-Based Water and Snow Indices for Extracting Lake and Snow Cover/Glacier in the Tibetan Plateau. Water, 12(5), 1339. https://doi.org/10.3390/w12051339

Yap Arévalo, A. A. (2016). Análisis multitemporal de glaciares y lagunas glaciares en la Cordillera Blanca e identificación de potenciales amenazas GLOFs. https://tesis.pucp.edu.pe/repositorio/handle/20.500.12404/7268